Advanced Pharmaceutical and Biomedical Letters
Available online at https://advpbl.org.ng
Adv Pharm Biomed Lett, 2026:3, 101-113

AdvPBL

Open Access Full Text Article

Original Article

Molecular Docking and ADMET Prediction of *Piper guineense* and *Telfairia occidentalis* Phytoconstituents Targeting DPP-4 and PPARγ Receptors

Kluvet O. Owowenu[1], Uyi M. Ogbeide[2*]

[1]Damilola Pharmacy, 2 Ahmed Bola Tinubu Way, Off Station Bus Stop, Fagba, Iju, Lagos State, Nigeria; [2]Department of Pharmaceutical Chemistry, Faculty of Pharmacy, University of Benin, Benin City, Edo State, Nigeria.
**Correspondence: uyi.ogbeide@uniben.edu Tel: +2347038058676*

Received 13 August 2026 Revised 20 October 2026 Accepted 21 October 2026 Published 23 November 2026

Copyright © 2026 the authors. This is an open access article distributed under the Creative Commons Attribution License which permits unrestricted use, distribution, and reproduction in any medium, provided the original work is properly cited. ***ISSN (online: 3093-0715; print: 3093-0723)***

Cite: *Owowenu KO, Ogbeide UM, 2026. Molecular Docking and ADMET Prediction of Piper guineense and Telfairia occidentalis Phytoconstituents Targeting DPP-4 and PPARγ Receptors. Advanced Pharmaceutical and Biomedical Letters, 3(1): 101-113. https://doi.org/10.59493/advpbl/2026.1.11*

Abstract

Diabetes mellitus remains a leading non-communicable metabolic disorder worldwide, driving continued interest in affordable, effective, and safe therapeutic agents from indigenous medicinal plants. This study aims to evaluate the antidiabetic potential of phytoconstituents from *Piper guineense* (uziza) and *Telfairia occidentalis* (fluted pumpkin) targeting dipeptidyl peptidase-4 (DPP-4, PDB ID: 4FFW) and peroxisome proliferator-activated receptor gamma (PPARγ, PDB ID: 5Y2O), two validated antidiabetic drug targets, using in silico methods. Phytoconstituents from both plants were retrieved from PubChem and docked against DPP-4 and PPARγ crystal structures using PyRx, with sitagliptin and pioglitazone as reference ligands. Receptor-ligand interactions were analyzed with BIOVIA Discovery Studio Visualizer 2020. SwissADME and ADMETLab were used to analyze the pharmacokinetic and toxicity profiles of ligands with binding affinity comparable to the reference ligands. Of the 125 P. guineense and 77 *T. occidentalis* phytoconstituents docked, 14 and 8, respectively, showed binding affinities equal or superior to the standards. Notably, gamma-tocopherol and a related dihydrochromenol derivative, both from *P. guineense*, showed binding affinities for DPP-4 (-9.9 kcal/mol) and PPARγ (-10.7 kcal/mol) exceeding sitagliptin (-8.4 kcal/mol) and pioglitazone (-8.8 kcal/mol). Most ligands satisfied Lipinski's Rule of Five with zero violations, though several tocopherol-related compounds showed high lipophilicity. Toxicity predictions were mixed, with the *P. guineense* tocopherol-related compounds showing the most favorable safety profiles. Phytoconstituents of both *P. guineense* and *T. occidentalis* show promising antidiabetic potential targeting DPP-4 and PPARγ, with *P. guineense* tocopherol-related compounds emerging as the leading candidates, warranting further in vitro and in vivo validation as candidate antidiabetic leads.

Keywords: Antidiabetic, DPP-4, In silico, Molecular docking, Phytoconstituents, PPARγ

Introduction

Diabetes mellitus is a chronic metabolic disorder characterized by persistent hyperglycemia arising from defects in insulin secretion, insulin action, or both [1], and is associated with severe long-term complications including cardiovascular disease, nephropathy, neuropathy, and retinopathy [2]. According to the International Diabetes Federation (2025), approximately 589 million adults aged 20-79 years are living with diabetes globally [3], a figure projected to rise substantially, particularly in low- and middle-income countries where access to affordable therapeutic options remains limited.

Current pharmacological management of type 2 diabetes mellitus includes several drug classes, among which dipeptidyl peptidase-4 (DPP-4) inhibitors and peroxisome proliferator-activated receptor gamma (PPARγ) agonists occupy an important place. DPP-4 inhibitors, such as sitagliptin, prevent the rapid degradation of incretin hormones, prolonging glucose-dependent insulin secretion and suppressing glucagon release [4,5]. PPARγ agonists, such as pioglitazone, act on a nuclear receptor that regulates gene transcription involved in adipocyte differentiation and insulin sensitization in muscle, liver, and adipose tissue [6]. Although clinically effective, these agents are associated with adverse effects, including gastrointestinal disturbances, weight gain, fluid retention, and, in some cases, increased cardiovascular risk, driving continued interest in safer alternatives from natural sources [7]. Medicinal plants have long served as reservoirs of bioactive phytoconstituents with therapeutic relevance, and

several indigenous Nigerian vegetables have documented ethnomedicinal use in diabetes management. *Piper guineense* ("Schumach. & Thonn."), commonly called uziza, is a pungent leafy spice rich in alkaloids, flavonoids, essential oils, and lignans, traditionally valued for its digestive, antimicrobial, and anti-inflammatory properties [8]. *Telfairia occidentalis* (Hook. f.), known as fluted pumpkin, is a widely consumed West African leafy vegetable traditionally reputed as a blood tonic and reported to lower blood glucose and improve glucose tolerance [9, 10]. Despite these traditional claims, the specific phytoconstituents responsible for antidiabetic activity, and their mechanistic interaction with validated drug targets such as DPP-4 and PPARγ, remain poorly characterized at the molecular level.

Molecular docking is a widely applied computational technique in drug discovery that predicts the preferred orientation of a small molecule (ligand) within a target protein's binding pocket and estimates the free energy of binding of the resulting complex [11]. It allows rapid, low-cost screening of large numbers of phytoconstituents against therapeutically relevant targets prior to more expensive in vitro and in vivo validation [12], and, coupled with prediction of absorption, distribution, metabolism, excretion, and toxicity (ADMET) properties, provides a rational basis for prioritizing candidate phytoconstituents for further drug development [12, 13].

This study, therefore, aims to evaluate *in silico* the antidiabetic potential of the phytoconstituents of *P. guineense* and *T. occidentalis* by molecular docking against DPP-4 (PDB ID: 4FFW) and PPARγ (PDB ID: 5Y2O), with the goal of identifying and characterizing the active-site interactions, pharmacokinetic properties, and toxicity profiles of promising lead compounds from both plants.

Materials and Methods

Materials

The materials employed in this in silico investigation included a computer workstation, the RCSB Protein Data Bank (https://rcsb.org) for retrieval of protein target structures, the PubChem database [14] for retrieval of phytoconstituent structures, PyRx version 0.8 [15] (incorporating Autodock Vina [16] and the Open Babel plug-in [17]) for virtual screening and molecular docking, PyMOL for identification of binding site amino acid residues, BIOVIA Discovery Studio Visualizer 2020 for post-docking interaction analysis, and the SwissADME and ADMETLab web servers for prediction of pharmacokinetic and toxicity properties, respectively [18, 19].

Identification and preparation of protein targets

The three-dimensional crystal structures of dipeptidyl peptidase-4 in complex with sitagliptin (PDB ID: 4FFW) and peroxisome proliferator-activated receptor gamma in complex with pioglitazone (PDB ID: 5Y2O) were retrieved from the RCSB Protein Data Bank (accessed 23 August, 2025) [20, 21].

Dipeptidyl peptidase-4 (DPP-4; PDB: 4FFW, with sitagliptin) and peroxisome proliferator-activated receptor gamma (PPARγ; PDB: 5Y2O, with pioglitazone) were selected to represent two clinically validated, mechanistically distinct antidiabetic pathways — incretin-based glucose regulation and insulin sensitization — enabling assessment of dual-target antidiabetic potential. Both structures are human, co-crystallized with a known reference ligand, and have well-characterized binding sites permitting docking-protocol validation by redocking of the native ligand. Non-standard residues, co-crystallized water molecules, and extraneous chains not relevant to docking were removed from each structure (chain A retained for both) using BIOVIA Discovery Studio, hydrogens were added, and the prepared structures were saved in PDB format for docking.

Identification and preparation of ligands

Phytoconstituents of *P. guineense* (125) were retrieved from PubChem [14] in structure data file (SDF) format; phytoconstituents of *T. occidentalis* (77) were identified from the literature [22,23] and likewise retrieved from PubChem in SDF format, then imported into PyRx via the Open Babel plug-in [15, 17]. Duplicate ligands sharing a PubChem CID were removed, and the remaining ligands were energy-minimized (UFF force field, 100 steps, conjugate gradients) before conversion to Protein Data Bank, Partial Charge, and Atom Type (pdbqt) format for docking with Autodock Vina [16], with four torsional degrees of freedom defined.

Identification of binding site

Binding-site amino acid residues for DPP-4 (4FFW) and PPARγ (5Y2O) were identified in PyMOL from the position of the co-crystallised reference ligands, sitagliptin and pioglitazone, respectively, using visual inspection and a distance cut-off, and validated against CASTp. Residues identified for DPP-4 were ARG123, GLU203, GLU204, ILE205, PHE206, GLY207, PHE355, ARG356, TYR548, SER631, TYR632, TRP660, TYR663, TYR667, and HIS741; for PPARγ, ILE281, PHE282, GLY284, CYS285, GLN286, ARG288, SER289, HIS323, ILE326, TYR327, LEU330, VAL339, ILE341, MET348, LEU353, PHE363, MET364, HIS449, LEU453, LEU469, and TYR473.

Molecular docking and post-docking analysis

The prepared protein targets were imported into PyRx and converted into macromolecules, and all prepared ligands were imported for docking. The grid box for each receptor was centered on the previously identified binding-site residues, and docking was performed using the Autodock Vina plug-in at an exhaustiveness of 8. Grid box dimensions are given in Tables 1 and 2 below.

Table 1: Grid box dimensions for 4FFW

	X	Y	Z
Measurement	19.5985	-10.1344	52.1378
Dimensions (Angstrom)	27.2726	21.0459	20.5279

Table 2: Grid box dimensions for 5Y2O

	X	Y	Z
Measurement	-47.8030	-1.0209	79.5359
Dimensions (Angstrom)	20.73396	22.5785	24.1793

Following docking, the co-crystallized ligands were re-docked to validate the protocol. Binding affinities of all ligands were retrieved and compared with the respective standard (sitagliptin for DPP-4; pioglitazone for PPARγ); ligands with affinities equal to or more negative than the standard were considered computationally prioritized candidates for further investigation. Docked poses were examined in BIOVIA Discovery Studio Visualizer 2020 to identify bond types (conventional hydrogen bonds, Pi-alkyl, Pi-sigma, Pi-Pi stacked, and carbon-hydrogen bonds) formed with binding-site residues.

Docking validation and accuracy measurement

As a validation step, the co-crystallized ligands were removed from each prepared receptor and re-docked under conditions identical to those used for the phytoconstituents (same grid box, exhaustiveness, and scoring function), to assess how accurately the protocol reproduced the known crystallographic binding pose. Accuracy was quantified as root-mean-square deviation (RMSD) between the re-docked and crystallographic poses, with RMSD ≤2.0 Å considered acceptable [24]. Both native ligands showed strong agreement with their crystal poses, supporting the protocol's suitability for the subsequent phytoconstituent screening.

ADMET profiling

Pharmacokinetic (absorption, distribution, metabolism, and excretion) properties of the docked phytoconstituents were predicted using the SwissADME web server (accessed 6 September, 2025), with compliance to Lipinski's Rule of Five (molecular weight ≤500 g/mol, hydrogen bond donors ≤5, hydrogen bond acceptors ≤10, and consensus Log Po/w ≤5) used as an indicator of drug-likeness [12]. Toxicity endpoints, including carcinogenicity, genotoxicity, hematotoxicity, nephrotoxicity, neurotoxicity, ototoxicity, and respiratory toxicity, were predicted using the ADMETLab web server (accessed 6 September, 2025) on a 0-1 scale, with scores closer to zero indicating a lower predicted likelihood of toxicity [19].

Data analysis

Docking results were organised in tabular form and ranked from most negative to least negative predicted binding affinity for each target. Ligands were compared against their standard/reference drug on the basis of binding affinity and the number and type of interactions formed with binding-site residues.

Results

Molecular docking analysis

Fourteen (14) compounds of *P. guineense* (compared with the standard ligands sitagliptin and pioglitazone) bound with varying affinities to DPP-4 and PPARγ, as shown in Table 3. Eight compounds of *T. occidentalis* (compared with the standard ligands) bound with varying affinities to the same targets, as shown in Table 4. Six of these eight compounds, those with a reported binding affinity at either target, were carried forward for ADMET profiling. The chemical structures of the standard ligands, sitagliptin and pioglitazone, are shown in Figure 3. The structures of the hit ligands from *P. guineense* (A–N) are shown in Figure 4, and those of the hit ligands from *T. occidentalis* (A–F) are shown in Figure 5.

ADME profiling

The ADME properties of the docked phytoconstituents from *Piper guineense* and *Telfairia occidentalis* are presented in Tables 5-8 below. All 14 hit compounds and both standard ligands satisfied Lipinski's Rule of Five with zero violations, but predicted gastrointestinal (GI) absorption probabilities were uniformly low (0.000–0.003) and consensus lipophilicity varied widely across the set, from 1.82 (covi-ox) to 9.48 (CID 162951652) (Table. 5). Most of the lignan-type compounds showed a high predicted probability (≥0.85) of inhibiting CYP1A2, CYP2C19, CYP2D6, CYP3A4 and CYP2B6, whereas covi-ox showed the opposite pattern — negligible inhibition of these five isoforms but a high probability of CYP2C8 inhibition (0.988) (Table. 6). As with *P. guineense*, all six *T. occidentalis* hit compounds satisfied Lipinski's Rule of Five, but consensus LogPo/w was elevated across the set (5.22–7.85) and predicted GI absorption probability was uniformly low (0.000), as shown in the Table 7.

Unlike the *P. guineense* hits, none of the *T. occidentalis* compounds showed appreciable CYP1A2 inhibition, but several showed a high probability of CYP2C8 and/or CYP2B6 inhibition, with ergost-5-en-3-ol and friedelin showing the broadest inhibition profiles, as shown in Table 8.

Table 3: Binding affinities (kcal/mol) of *Piper guineense* phytoconstituents against DPP-4 (4FFW) and PPARγ (5Y2O)

Compound	PubChem CID	4FFW	5Y2O
Sitagliptin*	4369359	-8.4	-
Pioglitazone*	4829	-	-8.8
Cubebin	117443	-8.4	-9.0
O-Ethylcubebin	13939336	-	-9.3
(2S,3S,4S)-3,4-bis(1,3-benzodioxol-5-ylmethyl)oxolan-2-ol	14137604	-8.8	-9.1
[(1R,2R,4aS,8aS)-2-(1,3-benzodioxol-5-yl)octahydronaphthalen-1-yl]-pyrrolidin-1-ylmethanone	162951652	-8.6	-
5-[[(2S,3S,4S)-4-(1,3-benzodioxol-5-ylmethyl)-2-ethoxyoxolan-3-yl]methyl]-1,3-benzodioxole	162953580	-8.4	-8.9
Alpha-cubebin	25021463	-	-9.0
Rac-cubebin	287685	-8.8	-
Hinokinin	442879	-	-9.4
23,24-Dihydrocucurbitacin F	54747446	-9.3	-
Covi-ox	6560141	-9.5	-9.5
5-[(3R,3aS,6S,6aR)-3-(1,3-benzodioxol-5-yl)hexahydrofuro[3,4-c]furan-6-yl]-1,3-benzodioxole	7059611	-9.2	-9.2
Sesamin	72307	-9.2	-9.2
(2S)-2,7,8-trimethyl-2-[(4S,8S)-4,8,12-trimethyltridecyl]-3,4-dihydrochromen-6-ol	73416557	-9.9	-10.7
Gamma-Tocopherol	92729	-9.9	-10.6

NOTE: ** denotes standard/reference ligand; "-" denotes binding affinity value not within the top-ranked docking output for that receptor.*

Table 4: Binding affinities (kcal/mol) of *Telfairia occidentalis* phytoconstituents against DPP-4 (4FFW) and PPARγ (5Y2O)

Compound	PubChem CID	4FFW	5Y2O
Sitagliptin*	4369359	-8.4	-
Pioglitazone*	4829	-	-8.8
Ergost-5-en-3-ol	18660356	-	-8.8
(23E)-14-Methylergosta-8,23-dien-3-ol	23258268	-	-
Clionasterol	457801	-8.5	-
4,22-Stigmastadiene-3-one	5364563	-	-
7,22-Ergostadienol	5319548	-8.9	-
Beta-amyron	612782	-9.0	-
Friedelin	91472	-9.4	-8.9
24-Methylenecycloartanol	94204	-	-

*NOTE: * denotes standard/reference ligand; "-" denotes binding affinity value not within the top-ranked docking output for that receptor.*

Table 5: Physicochemical Properties & Absorption/Transport of *Piper guineense* Phytoconstituents

PubChem CID	MW (g/mol)	H-Bond Acceptors	H-Bond Donors	Consensus LogPo/w	Lipinski (violations)	TPSA (Ų)	GI Absorption	BBB Permeability	P-gp Inhibitor	P-gp Substrate
117443	356.13	6	1	2.51	0	66.38	0.000	0.802	0.923	0.026
13939336	384.16	6	0	2.97	0	55.38	0.000	0.998	0.822	0.002
14137604	356.13	6	1	2.35	0	66.38	0.000	0.850	0.870	0.021
162951652	430.38	2	1	9.48	0	29.46	0.000	0.987	0.041	0.001
162953580	353.20	4	0	3.70	0	38.77	0.000	0.629	0.565	0.142
25021463	384.16	6	0	2.85	0	55.38	0.000	0.988	0.835	0.006
287685	356.13	6	1	2.43	0	66.38	0.000	0.982	0.783	0.029
442879	356.13	6	1	2.50	0	66.38	0.000	0.987	0.788	0.020
54747446	354.11	6	0	2.50	0	63.22	0.000	0.564	0.829	0.004
6560141	520.34	7	5	1.82	0	135.29	0.003	0.721	0.000	0.157
7059611	430.38	2	1	9.35	0	29.46	0.000	1.000	0.000	0.002
72307	354.11	6	0	2.19	0	55.38	0.000	0.978	0.282	0.001
73416557	354.11	6	0	2.30	0	55.38	0.000	0.998	0.328	0.003
92729	416.37	2	1	8.97	0	29.46	0.000	0.999	0.000	0.004
117443	416.37	2	1	8.90	0	29.46	0.000	0.961	0.002	0.004

Table 6: Cytochrome P450 Inhibition Profile of *Piper guineense* Phytoconstituents

PubChem CID	CYP1A2 Inhibitor	CYP2C19 Inhibitor	CYP2C9 Inhibitor	CYP2D6 Inhibitor	CYP3A4 Inhibitor	CYP2B6 Inhibitor	CYP2C8 Inhibitor
117443	1.000	0.964	0.744	1.000	1.000	1.000	0.000
13939336	0.990	0.992	0.825	1.000	1.000	1.000	0.000
14137604	1.000	0.994	0.901	1.000	1.000	1.000	0.000
162951652	0.254	1.000	1.000	0.023	0.870	1.000	1.000
162953580	0.036	0.956	0.168	0.791	0.997	1.000	0.079
25021463	1.000	0.999	0.793	1.000	1.000	1.000	0.001
287685	1.000	0.987	0.901	1.000	1.000	1.000	0.000
442879	0.999	0.850	0.675	1.000	1.000	1.000	0.000
54747446	0.999	0.986	0.982	1.000	1.000	1.000	0.012
6560141	0.000	0.000	0.033	0.000	0.002	0.355	0.988
7059611	0.431	0.999	0.990	0.020	0.706	1.000	1.000
72307	1.000	0.995	0.439	1.000	1.000	1.000	0.000
73416557	1.000	0.997	0.393	1.000	1.000	1.000	0.000
92729	0.712	1.000	0.999	0.140	0.635	1.000	1.000
117443	0.371	1.000	1.000	0.038	0.918	1.000	1.000

Table 7: Physicochemical Properties & Absorption/Transport of *Telfairia occidentalis* phytoconstituents

PubChem CID	MW (g/mol)	H-Bond Acceptors	H-Bond Donors	Consensus LogPo/w	Lipinski (violations)	TPSA (Ų)	GI Absorption	BBB Permeability	P-gp Inhibitor	P-gp Substrate
18660356	400.37	1	1	7.56	0	20.23	0.000	0.258	0.001	0.044
457801	414.39	1	1	7.85	0	20.23	0.000	0.060	0.000	0.078
5364563	410.35	1	0	6.03	0	17.07	0.000	0.791	0.730	0.000
5319548	398.35	1	1	6.84	0	20.23	0.000	0.035	0.693	0.000
612782	424.37	1	0	6.25	0	17.07	0.000	0.967	0.984	0.000
91472	426.39	1	0	5.22	0	17.07	0.000	0.522	1.000	0.000

Table 8: Cytochrome P450 Inhibition Profile of *Telfairia occidentalis* phytoconstituents

PubChem CID	CYP1A2 Inhibitor	CYP2C19 Inhibitor	CYP2C9 Inhibitor	CYP2D6 Inhibitor	CYP3A4 Inhibitor	CYP2B6 Inhibitor	CYP2C8 Inhibitor
18660356	0.000	0.004	0.422	0.519	0.179	1.000	**1.000**
457801	0.000	0.000	0.103	0.225	0.075	1.000	**0.999**
5364563	0.000	0.099	0.018	0.000	0.000	0.001	**0.182**
5319548	0.000	0.211	0.912	0.000	0.550	0.007	**0.833**
612782	0.000	0.141	0.429	0.003	0.521	0.027	**0.994**
91472	0.000	0.304	0.181	0.011	0.135	1.000	**0.955**

MW — Molecular Weight; LogPo/w — Logarithm of the octanol-water partition coefficient (a measure of lipophilicity). "Consensus" indicates ADMETLab3's consensus-predicted value; Lipinski — Number of violations of Lipinski's Rule of Five (a rule-of-thumb for drug-likeness); TPSA — Topological Polar Surface Area, measured in Ų (square Ångströms); GI Absorption — Predicted probability of human intestinal absorption (HIA); BBB — Blood-Brain Barrier (permeability is the predicted probability the compound crosses it); P-gp — P-glycoprotein, an efflux transporter; values show the predicted probability the compound is an inhibitor or a substrate of it; CYP — Cytochrome P450, a family of liver drug-metabolizing enzymes; values show the predicted probability the compound inhibits each isoform (1A2, 2C19, 2C9, 2D6, 3A4, 2B6, 2C8); All probability values (GI Absorption, BBB, P-gp, CYP columns) are ADMETLab3 model output scores ranging from 0 to 1, representing the predicted probability that the compound is positive for that endpoint.

Table 9: Toxicity prediction of *Piper guineense* phytoconstituents

PubChem CID	Carcinogenicity	Genotoxicity	Hematotoxicity	Nephrotoxicity	Neurotoxicity	Ototoxicity	Respiratory Toxicity
117443	0.5294	0.9863	0.4468	0.8763	0.7064	0.7901	0.6657
13939336	0.5676	0.3047	0.3752	0.5674	0.6573	0.8288	0.5761
14137604	0.7235	0.9491	0.4171	0.8616	0.8163	0.7171	0.4765
162951652	0.5859	0.0000	0.1520	0.2306	0.0146	0.5411	0.8247
162953580	0.8170	0.0124	0.6099	0.5028	0.1434	0.2212	0.7698
25021463	0.7464	0.9470	0.4561	0.8345	0.8159	0.5090	0.3673
287685	0.8356	0.9954	0.6921	0.9516	0.9450	0.7272	0.6007
442879	0.5351	0.3035	0.3530	0.5941	0.7194	0.9333	0.5844
54747446	0.9205	0.9968	0.7317	0.9154	0.8531	0.6087	0.2247
6560141	0.6308	0.6223	0.4775	0.6400	0.0425	0.8610	0.3889
7059611	0.7592	0.0001	0.2948	0.2333	0.0149	0.4531	0.7745
72307	0.8777	0.8361	0.5867	0.5520	0.3738	0.2083	0.3973
73416557	0.9031	0.9428	0.4870	0.6301	0.5439	0.2656	0.4019
92729	0.7048	0.0001	0.2834	0.2568	0.0145	0.4554	0.7444
117443	0.4527	0.0001	0.1545	0.2482	0.0313	0.5186	0.8804

Table 10: Toxicity prediction of *Telfairia occidentalis* phytoconstituents

PubChem CID	Carcinogenicity	Genotoxicity	Hematotoxicity	Nephrotoxicity	Neurotoxicity	Ototoxicity	Respiratory Toxicity
18660356	0.8252	0.0053	0.4569	0.5940	0.0948	0.5724	0.7638
457801	0.7516	0.0017	0.2864	0.6849	0.1221	0.4252	0.3943
5364563	0.4122	0.0049	0.1957	0.0748	0.7161	0.7937	0.6972
5319548	0.2028	0.0003	0.0674	0.0529	0.5108	0.8851	0.7508
612782	0.3804	0.0056	0.2574	0.0831	0.5827	0.7764	0.7460
91472	0.8996	0.7604	0.5945	0.8387	0.2417	0.3791	0.7419

Table 11: Active site interactions for *Piper guineense* ligands

	4FFW (DPP-4)		5Y2O (PPARγ)	
Ligand	Active Site Amino Acid	Type of Bond	Active Site Amino Acid	Type of Bond
72307	TYR548	Conventional hydrogen bond	-	-
92729	ILE205	Conventional hydrogen bond	ILE326	Conventional hydrogen bond
117443	GLN554, TRP630	Conventional hydrogen bond	SER342	Conventional hydrogen bond
287685	GLU203, SER631	Conventional hydrogen bond	-	-
6560141	-	-	-	-
7059611	TYR548	Conventional hydrogen bond	-	-
14137604	GLN554, TRP630	Conventional hydrogen bond	CYS285, SER342	Conventional hydrogen bond
54747446	TYR548, SER631, TYR632, ARG670	Conventional hydrogen bond	-	-
73416557	ILE205	Conventional hydrogen bond	LEU340	Conventional hydrogen bond
162951652	TYR548	Conventional hydrogen bond	-	-
442879	-	-	SER342, TYR327	Conventional hydrogen bond
13939336	-	-	TYR327	Conventional hydrogen bond
25021463	-	-	SER342	Conventional hydrogen bond
162953580	-	-	SER342	Conventional hydrogen bond

Table 12: Active site interactions for ligands from *Telfairia occidentalis*

	4FFW (DPP-4)		5Y2O (PPARγ)	
Ligands	Active site amino acids	Type of bond	Active site amino acids	Type of bond
91472	-	-	-	-
457801	TYR663	Conventional hydrogen bond	-	-
612782	-	-	-	-
5319548	GLU204	Conventional hydrogen bond	-	-
5364563	-	-	-	-
18660356	-	-	ARG280	Conventional hydrogen bond

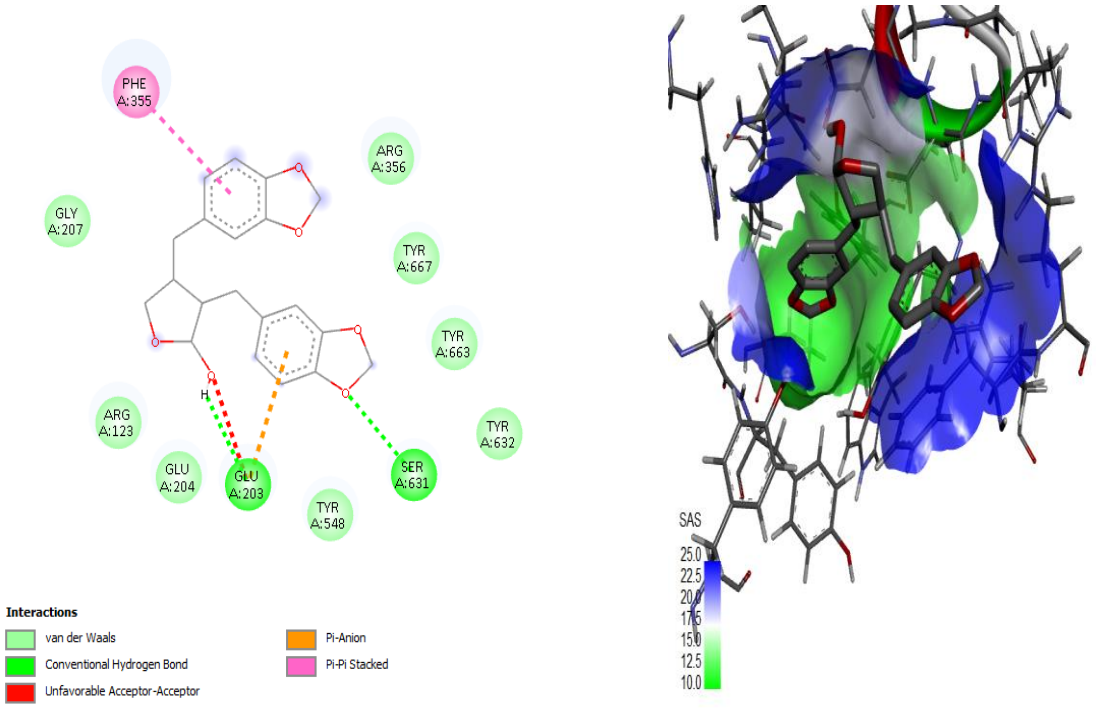

A B

Figure 1: (A) Two-dimensional and (B) three-dimensional interaction profile of PubChem CID 287685 with 4FFW showing hydrogen bonding and hydrophobic interactions.

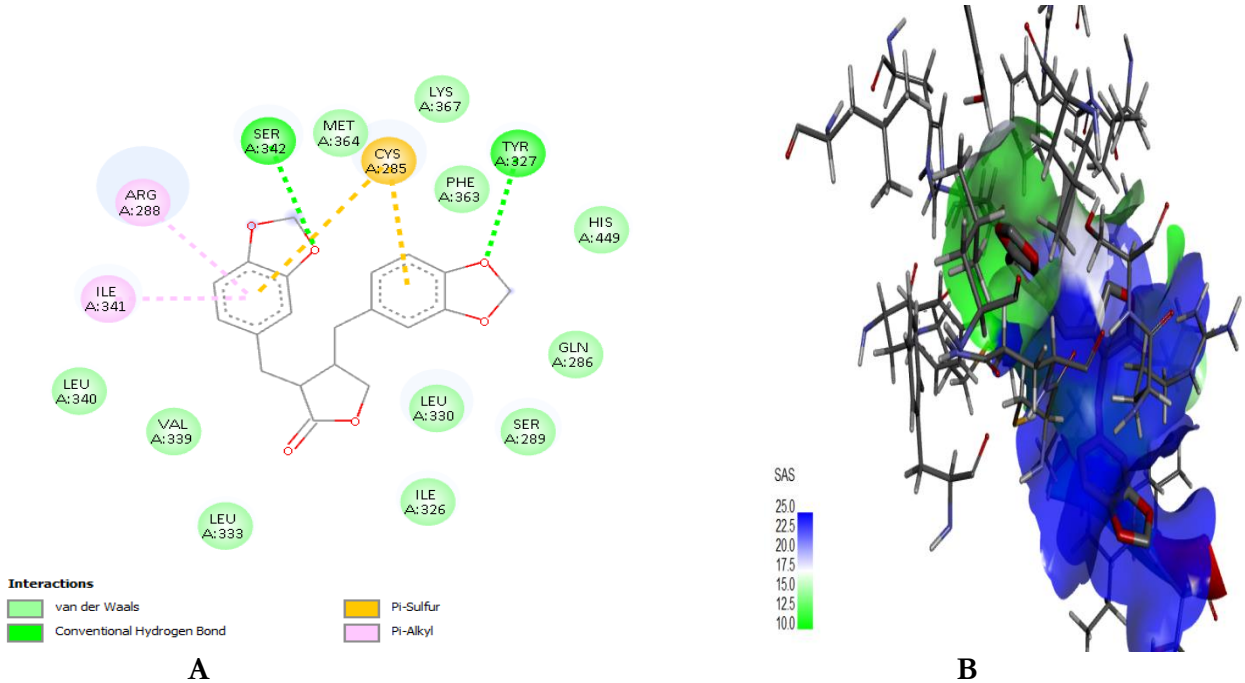

A B

Figure 2: (A) Two-dimensional and (B) three-dimensional interaction profile of PubChem CID 442879 with 5Y2O receptor showing hydrogen bonding and hydrophobic interactions.

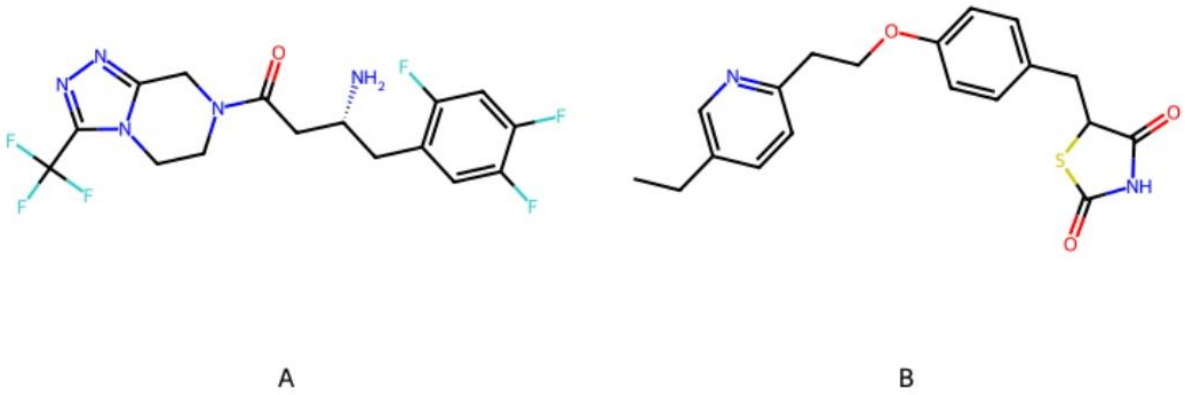

Figure 3. Chemical structures of the standard ligands. A = Sitagliptin; B = Pioglitazone.

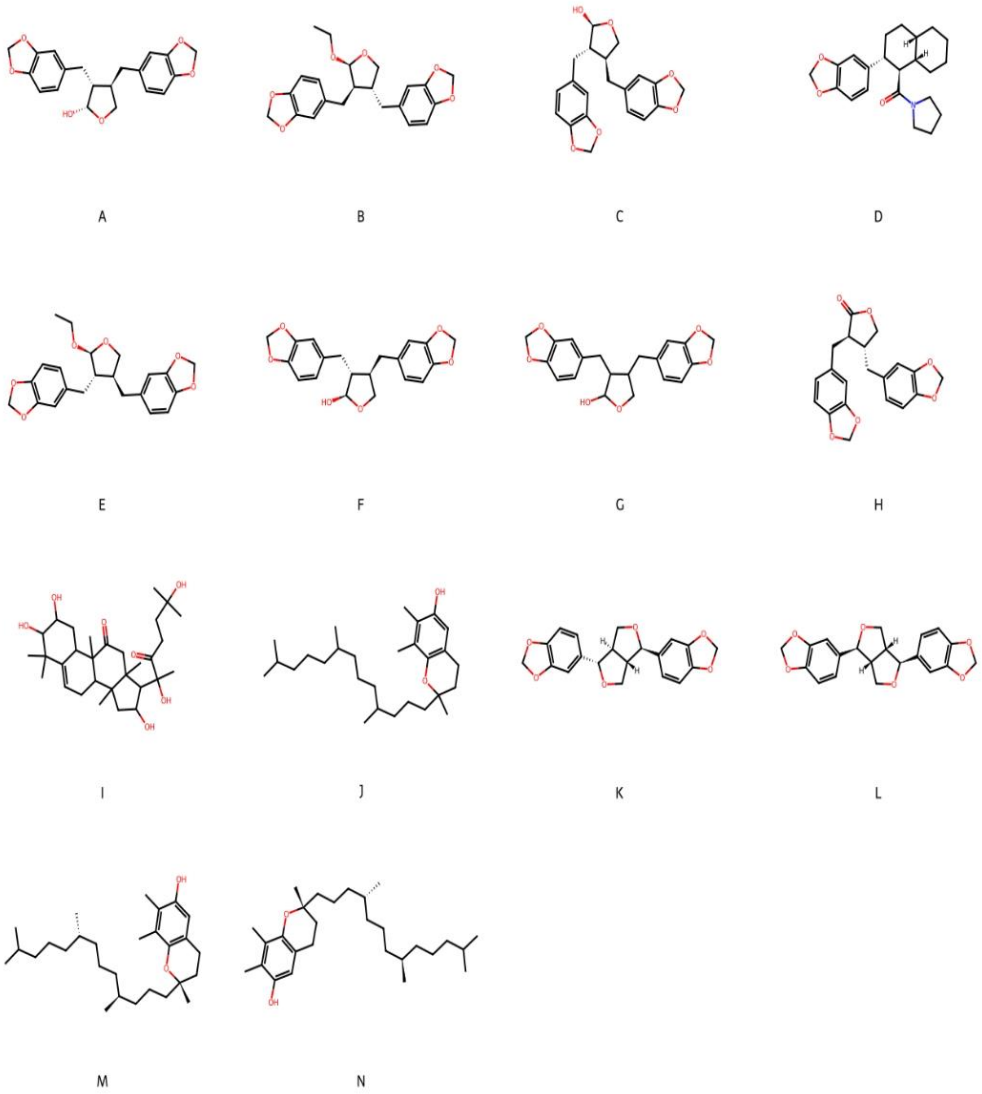

Figure 4: Chemical structures of the hit ligands from *Piper guineense*

A = Cubebin; B = O-Ethylcubebin; C = (2S,3S,4S)-3,4-bis(1,3-benzodioxol-5-ylmethyl)oxolan-2-ol; D = [(1R,2R,4aS,8aS)-2-(1,3-benzodioxol-5-yl)octahydronaphthalen-1-yl]-pyrrolidin-1-ylmethanone; E = 5-[[(2S,3S,4S)-4-(1,3-benzodioxol-5-ylmethyl)-2-ethoxyoxolan-3-yl]methyl]-1,3-benzodioxole; F = Alpha-cubebin; G = Rac-cubebin; H = Hinokinin; I = 23,24-Dihydrocucurbitacin F; J = Covi-ox; K = 5-[(3R,3aS,6S,6aR)-3-(1,3-benzodioxol-5-yl)hexahydrofuro[3,4-c]furan-6-yl]-1,3-benzodioxole; L = Sesamin; M = (2S)-2,7,8-trimethyl-2-[(4S,8S)-4,8,12-trimethyltridecyl]-3,4-dihydrochromen-6-ol; N = Gamma-Tocopherol.

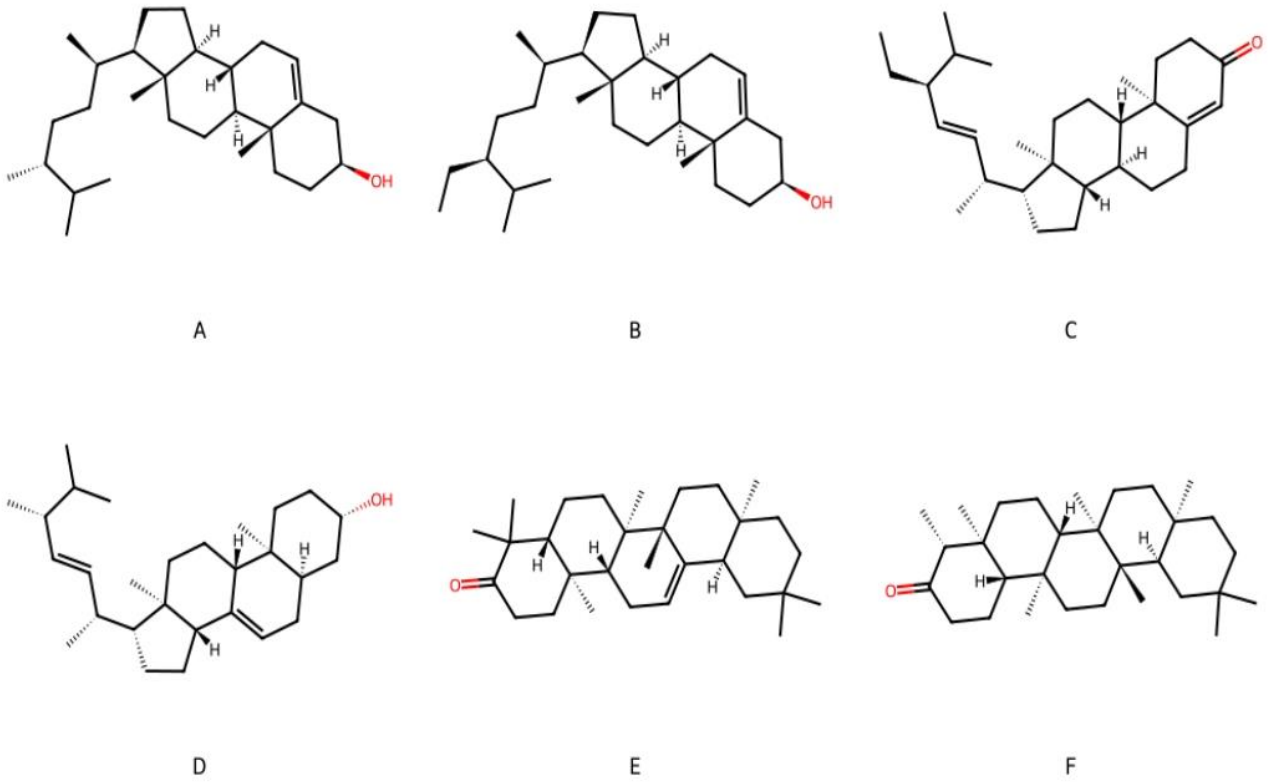

Figure 5: Chemical structures of hit ligands from *Telfairia occidentalis*.
A = Ergost-5-en-3-ol; B = Clionasterol; C = 4,22-Stigmastadiene-3-one; D = 7,22-Ergostadienol; E = Beta-amyron; F = Friedelin.

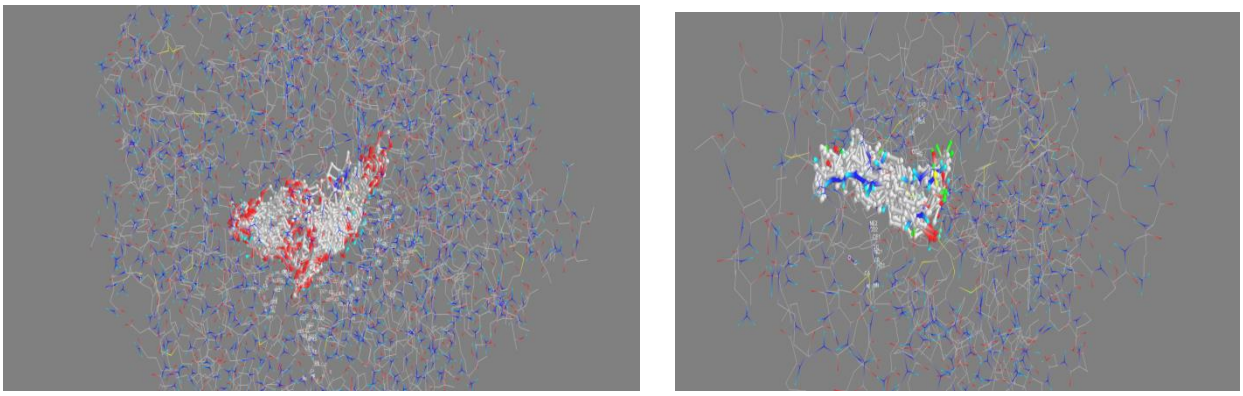

Figure 6: Docking Validation for 4FFW and 5Y2O.
A = Docking validation for 4FFW receptor with rmsd value of zero for all ligands including the reference ligand; B = Docking validation for 5Y2O receptor with rmsd value of zero for all ligands including the reference ligand.

Toxicity prediction

The predicted toxicity profiles (ranging from 0-1 with values closer to 0 as non-toxic and values closer to 1 as toxic) of the docked phytoconstituents from *Piper guineense* and *Telfairia occidentalis* are presented in Table 9 and Table 10, respectively. Hinokinin and alpha-cubebin recorded the highest carcinogenicity and genotoxicity probabilities among the *P. guineense* hits (both >0.8 on each endpoint), while gamma-tocopherol and the dihydrochromen-6-ol derivative recorded the lowest genotoxicity probabilities in the entire panel (≤0.0001), as detailed in the toxicity Tables 9-10.

Ligand interactions

Molecular interaction analysis with 4FFW and 5Y2O showed representative two- and three-dimensional binding patterns for selected compounds. Rac-cubebin (CID 287685) forms a single conventional hydrogen bond with SER631 at the DPP-4 site (Figure 1), whereas hinokinin (CID 442879) forms two conventional hydrogen bonds, with SER342 and TYR327, at the PPARγ site (Figure 2) — a more extensive polar anchoring pattern than seen for rac-cubebin at DPP-4. Only conventional hydrogen bonds are reported in Table 11; the fuller set of interaction types identified by BIOVIA Discovery Studio (also including Pi-alkyl, Pi-sigma, Pi-Pi stacked, and carbon-hydrogen contacts) is discussed further under Discussion. Table 11 shows the active-site interactions for the ligands from *Piper guineense* involving conventional hydrogen bonds. Table 12 shows the active-site interactions for the ligands from *Telfairia occidentalis*. Only three of the six hit compounds formed conventional hydrogen bonds: clionasterol (CID 457801) with TYR663 and 7,22-ergostadienol (CID 5319548) with GLU204 at DPP-4, and ergost-5-en-3-ol (CID 18660356) with ARG280 at PPARγ. Friedelin (CID 91472), beta-amyron (CID 612782) and 4,22-stigmastadiene-3-one (CID 5364563) formed none.

Discussion

Sitagliptin, the DPP-4 reference ligand, blocks incretin degradation (e.g., GLP-1), enhancing glucose-dependent insulin secretion and suppressing glucagon release [4,5]. Pioglitazone, the PPARγ reference, is a thiazolidinedione that activates the receptor and improves insulin sensitivity [6,7]. Their affinities (-8.4 kcal/mol at 4FFW; -8.8 kcal/mol at 5Y2O) served as benchmarks for the phytoconstituents.

Docking validation and interpretation of binding affinity

Re-docking of the native ligands reproduced the crystallographic poses (RMSD 0 Å for both receptors; Figure 6), within the ≤2.0 Å threshold [24]. This validates pose geometry, not affinity values. AutoDock Vina scores are empirical estimates that neglect receptor flexibility, explicit solvation, entropy and kinetics [11,25,26]; differences of 0.1-0.3 kcal/mol, as between several pairs in Tables 3 and 4, are unresolvable by docking, and even 1-2 kcal/mol gaps rarely scale reliably with potency. A recent review found that natural-product docking scores often fail to correlate with enzymatic potency and advised docking as a triage step only [27]. All comparisons below are therefore hypotheses, not confirmed differences in antidiabetic potency.

Binding profiles of the phytoconstituents

P. guineense compounds bound DPP-4 at -8.4 to -9.9 kcal/mol (Table 3). Gamma-tocopherol and its dihydrochromen-6-ol derivative (CID 73416557) scored highest (-9.9), comparable to rather than decisively better than sitagliptin, while cubebin and CID 162953580 matched it (-8.4); TYR548 and ARG356 were most frequently engaged. At PPARγ, all compounds (-8.9 to -10.7) met or exceeded pioglitazone, led by CID 73416557 (-10.7), gamma-tocopherol (-10.6), hinokinin (-9.4) and O-ethylcubebin (-9.3), mainly through TYR327 and ILE326, residues of the thiazolidinedione pocket. Interactions added nuance: rac-cubebin formed one hydrogen bond at DPP-4 (SER631), whereas hinokinin formed two at PPARγ (SER342, TYR327) (Figures 1-2).

T. occidentalis compounds bound DPP-4 at -8.4 to -9.4 kcal/mol, led by friedelin (-9.4), beta-amyron (-9.0) and 7,22-ergostadienol (-8.9) (Table 4); at PPARγ only ergost-5-en-3-ol and friedelin (-8.8, -8.9) approached pioglitazone. As shown in Table 12, only three of the six compounds formed a single conventional hydrogen bond (clionasterol–TYR663 and 7, 22-ergostadienol–GLU204 at DPP-4; ergost-5-en-3-ol–ARG280 at PPARγ), and friedelin, beta-amyron and 4, 22-stigmastadiene-3-one formed none at either target, consistent with their non-polar sterol and triterpenoid chemistry, showing that affinity rankings can conceal differences in binding quality.

ADME and cytochrome P450 profile

All 14 *P. guineense* and six *T. occidentalis* hits had zero Lipinski violations (Tables 5 and 7), but lipophilicity varied widely. Gamma-tocopherol (LogPo/w 8.97) and two lignan derivatives (CID 162951652, 9.48; CID 7059611, 9.35) would probably need lipid-based formulation, whereas covi-ox (1.82) and CID 73416557 (2.30) were far more favourable. Predicted GI absorption was near zero (0.000-0.003) for virtually every compound regardless of Lipinski compliance, qualifying any claim of oral bioavailability; this may be a genuine liability or a classifier artefact.

Cytochrome P450 predictions (Tables 6 and 8) revealed a further drug-interaction liability. Most *P. guineense* lignans and CID 73416557 showed high probability (≥0.85) of simultaneously inhibiting CYP1A2, CYP2C19, CYP2D6, CYP3A4 and CYP2B6, whereas covi-ox inhibited mainly CYP2C8 (0.988). Among *T. occidentalis* hits, ergost-5-en-3-ol and friedelin showed high CYP2B6/CYP2C8 inhibition, a caution for ergost-5-en-3-ol that toxicity screening alone would have missed.

Toxicity profile and lead prioritization

Applying a conventional threshold to the ADMETLab outputs (>0.7 high, 0.3-0.7 borderline, <0.3 low risk; Tables 9 and 10), hinokinin and alpha-cubebin exceeded 0.7 on five of seven endpoints, sesamin and two furan-type derivatives (CID 162953580, CID 7059611) on three or more, and friedelin on four despite its top DPP-4 affinity; ergost-5-en-3-ol and clionasterol crossed it on carcinogenicity alone. These should be deprioritized despite competitive docking scores. Gamma-tocopherol, CID 73416557 and covi-ox exceeded the threshold only for respiratory toxicity, a lone flag more plausibly a classifier false positive given the clinical safety of dietary tocopherols. The predictions are, however, only partly reliable: sesamin and hinokinin were negative in published genotoxicity assays [28,29] despite high in silico genotoxicity scores here, so such outputs are triage tools requiring in vitro confirmation.

Integrating all four data layers changes the ranking. Docking alone would rank CID 73416557, gamma-tocopherol, hinokinin and friedelin together, and Lipinski compliance would treat all twenty hits alike. Combined, CID 73416557 and covi-ox emerge as priority leads, pairing strong dual-target binding with modest

lipophilicity and sub-threshold toxicity (CID 73416557's CYP-inhibition signal still needs experimental checking); gamma-tocopherol is a close second but carries lipophilicity and CYP burdens. The remaining lignans and the *T. occidentalis* sterols and triterpenoids fail on toxicity and/or CYP inhibition despite comparable or better docking scores, so affinity, ADME and safety are only loosely correlated here.

Limitations of the study

This study is purely computational: none of the predicted affinities, pharmacokinetic properties or toxicity outcomes has been experimentally verified. Autodock Vina's rigid-receptor scoring only approximates binding free energy, and no molecular dynamics, MM-GBSA or per-residue energy decomposition was performed. Re-docking validated pose geometry, not affinity values. SwissADME and ADMETLab outputs are machine-learning estimates prone to false positives and negatives, as the sesamin and hinokinin genotoxicity discrepancy shows [28,29]. Only two targets and the PubChem-catalogued constituents of two species were examined, so the findings should not be generalized. Future work should include molecular dynamics refinement, in vitro enzyme and cell-based assays, and in vivo validation.

Conclusion

This study computationally screened phytoconstituents from *Piper guineense* and *Telfairia occidentalis* against DPP-4 and PPARγ. Fourteen *P. guineense* compounds and eight *T. occidentalis* compounds were reported with affinities comparable to or better than the reference ligands. CID 73416557 and gamma-tocopherol showed the strongest dual-target scores, while CID 73416557 and covi-ox had comparatively favourable combined predicted profiles. However, low predicted GI absorption and potential CYP/toxicity liabilities require caution. These findings identify candidates for further study, not confirmed antidiabetic agents; enzyme assays, cellular studies, molecular-dynamics analysis and *in vivo* validation are needed.

Declarations

Ethical approval
Ethical approval was not required for this study.

Informed consent
Not applicable.

Consent for publication
Not applicable.

Availability of data and materials
The datasets generated and/or analysed during the current study are available from the corresponding author upon reasonable request.

Conflict of interest
The authors declare that they have no competing interests.

Funding
This research received no specific grant from any funding agency in the public, commercial, or not-for-profit sectors.

Authors' contributions
UMO conceptualized the study, supervised the research, and reviewed the manuscript. KOO carried out the *in silico* experiments, analysed the data, and drafted the manuscript.

Acknowledgements
The authors sincerely acknowledge the Department of Pharmaceutical Chemistry, Faculty of Pharmacy, University of Benin, for providing the necessary resources and environment for this research.

Artificial Intelligence (AI) disclosure
The authors used Claude AI for language editing and grammar improvement. The authors reviewed and take full responsibility for the final content.

References

1. Goyal R, Singhal M, Jialal I, 2023. Type 2 diabetes. In: StatPearls. Treasure Island (FL): StatPearls Publishing. [Accessed 26th September, 2026]. Available: https://www.ncbi.nlm.nih.gov/books/NBK513253/
2. Kulkarni A, Thool AR, Daigavane S, 2024. Understanding the clinical relationship between diabetic retinopathy, nephropathy, and neuropathy: A comprehensive review. Cureus, 16(3): e56674. https://doi.org/10.7759/cureus.56674
3. Genitsaridi I, Salpea P, Salim A, Sajjadi SF, Tomic D, James S, Thirunavukkarasu S, Issaka A, Chen L, Basit A, Luk AOY, Ma RCW, Mbanya JC, Ramachandran A, Wild SH, Duncan BB, Boyko EJ, Magliano DJ, 2025. 11th edition of the IDF Diabetes Atlas: global, regional, and national diabetes prevalence estimates for 2024 and projections for 2050. The Lancet Diabetes & Endocrinology. https://doi.org/10.1016/S2213-8587(25)00299-2
4. Makrilakis K, 2019. The role of DPP-4 inhibitors in the treatment algorithm of type 2 diabetes mellitus: When to select, what to expect. International Journal of Environmental Research and Public Health, 16(15): 2720. https://doi.org/10.3390/ijerph16152720
5. Kasina SVSK, Baradhi KM, 2023. Dipeptidyl peptidase IV (DPP IV) inhibitors. In: StatPearls. Treasure Island (FL): StatPearls Publishing. [Accessed 26th September, 2026]. Available: https://www.ncbi.nlm.nih.gov/books/NBK542331/
6. Basak S, Murmu A, Matore BW, Roy PP, Singh J, 2024. Thiazolidinedione an auspicious scaffold as PPAR-γ agonist: its possible mechanism to manoeuvre against insulin resistant diabetes mellitus. European Journal of Medicinal Chemistry Reports, 11: 100160. https://doi.org/10.1016/j.ejmcr.2024.100160
7. Eggleton JS, Jialal I, 2023. Thiazolidinediones. In: StatPearls. Treasure Island (FL): StatPearls Publishing. [Accessed 26th September, 2026]. Available: https://www.ncbi.nlm.nih.gov/books/NBK551656/
8. Alagbe OA, Alagbe GO, Adekunle EA, Ayodele OO, Olorode EM, Oyediran RI, Oloyede EO, Oluwaloni FO, Oyeleye AO, 2021. Ethnomedicinal uses and therapeutic activities of Piper guineense: A review. Journal of Applied Sciences and Environmental Management, 25(6): 927-937. https://doi.org/10.4314/jasem.v25i6.6

9. Ojimelukwe PC, 2022. Telfairia occidentalis: A blood booster, an antioxidant and an antihyperglycaemic agent. International Journal of Food Science and Nutrition, 7(3): 1-9. Available: https://www.foodsciencejournal.com/assets/archives/2022/vol7issue3/7-3-13-398.pdf
10. Ugwu PN, Eze FI, Chukwube VO, Mgbeokwere CE, Ezenwanne DO, Ezea CC, Okonta EO, Odo EU, 2025. Pharmacognostic, phytochemical, antioxidant and toxicological properties of aqueous extract of Telfairia occidentalis Hook. F. leaves. Tropical Journal of Pharmaceutical Research, 24(4): 529-537. https://doi.org/10.4314/tjpr.v24i4.10
11. Dar AM, Mir S, 2017. Molecular docking: Approaches, types, applications, and basic challenges. Journal of Analytical and Bioanalytical Techniques, 8(2): 8-10. https://doi.org/10.4172/2155-9872.1000356
12. Asiamah I, Obiri SA, Tamekloe W, Armah FA, Borquaye LS, 2023. Applications of molecular docking in natural products-based drug discovery. Scientific African, 20: e01593. https://doi.org/10.1016/j.sciaf.2023.e01593
13. Kommalapati HS, Pilli P, Golla VM, Bhatt N, Samanthula G, 2023. In silico tools to thaw the complexity of the data: Revolutionizing drug research in drug metabolism, pharmacokinetics and toxicity prediction. Current Drug Metabolism, 24(11): 735-755. https://doi.org/10.2174/0113892002270798231201111422
14. Kim S, Chen J, Cheng T, Gindulyte A, He J, He S, Li Q, Shoemaker BA, Thiessen PA, Yu B, Zaslavsky L, Zhang J, Bolton EE, 2023. PubChem 2023 update. Nucleic Acids Research, 51(D1): D1373-D1380. https://doi.org/10.1093/nar/gkac956
15. Dallakyan S, Olson AJ, 2015. Small-molecule library screening by docking with PyRx. Methods in Molecular Biology, 1263: 243-250. https://doi.org/10.1007/978-1-4939-2269-7_19
16. Trott O, Olson AJ, 2010. AutoDock Vina: Improving the speed and accuracy of docking with a new scoring function, efficient optimization, and multithreading. Journal of Computational Chemistry, 31(2): 455-461. https://doi.org/10.1002/jcc.21334
17. O'Boyle NM, Banck M, James CA, Morley C, Vandermeersch T, Hutchison GR, 2011. Open Babel: An open chemical toolbox. Journal of Cheminformatics, 3: 33. https://doi.org/10.1186/1758-2946-3-33
18. Daina A, Michielin O, Zoete V, 2017. SwissADME: A free web tool to evaluate pharmacokinetics, drug-likeness, and medicinal chemistry friendliness of small molecules. Scientific Reports, 7: 42717. https://doi.org/10.1038/srep42717
19. Xiong G, Wu Z, Yi J, Fu L, Yang Z, Hsieh C, Yin M, Zeng X, Wu C, Lu A, Chen X, Hou T, Cao D, 2021. ADMETlab 2.0: An integrated online platform for accurate and comprehensive predictions of ADMET properties. Nucleic Acids Research, 49(W1): W5-W14. https://doi.org/10.1093/nar/gkab255
20. Berman HM, Westbrook J, Feng Z, Gilliland G, Bhat TN, Weissig H, Shindyalov IN, Bourne PE, 2000. The Protein Data Bank. Nucleic Acids Research, 28(1): 235-242. https://doi.org/10.1093/nar/28.1.235
21. Burley SK, Bhikadiya C, Bi C, Bittrich S, Chen L, Crichlow GV, Christie CH, Dalenberg K, Di Costanzo L, Duarte JM, Dutta S, Feng Z, Ganesan S, Goodsell DS, Ghosh S, Green RK, Guranović V, Guzenko D, Hudson BP, Lawson CL, Liang Y, Lowe R, Namkoong H, Peisach E, Persikova I, Randle C, Rose A, Rose Y, Sali A, Segura J, Sekharan M, Shao C, Tao YP, Voigt M, Westbrook JD, Young J, Zardecki C, Zhuravleva M, 2021. RCSB Protein Data Bank: powerful new tools for exploring 3D structures of biological macromolecules for basic and applied research and education in fundamental biology, biomedicine, biotechnology, bioengineering and energy sciences. Nucleic Acids Research, 49(D1): D437-D451. https://doi.org/10.1093/nar/gkaa1038
22. Eseyin OA, Zubaid M, Rathore HA, Aigbe F, Afzal S, Ahmad A, Lazhari M, Akhtar S, 2018. GC-MS and HPLC profiles of phenolic fractions of the leaf of Telfairia occidentalis. Pakistan Journal of Pharmaceutical Sciences, 31(1): 45-50.
23. Desire TC, Itoro EW, Itohowo OA, Ekemini TD, 2022. Antioxidant activity and identification of bioactive compounds in Telfairia occidentalis leaves using GC-MS analysis. World Journal of Advanced Research and Reviews, 16(3): 775-788. https://doi.org/10.30574/wjarr.2022.16.3.1291
24. Ogbeide UM, Owowenu KO, 2026. In silico evaluation of the antidiarrhoeal potential of phytoconstituents from Vernonia amygdalina, Ocimum gratissimum and Piper guineense. Nigerian Journal of Pharmaceutical and Applied Science Research, 15(2): 7-22. https://doi.org/10.60787/nijophasr-v15-i2-649
25. Ferreira LG, dos Santos RN, Oliva G, Andricopulo AD, 2015. Molecular docking and structure-based drug design strategies. Molecules, 20(7): 13384-13421. https://doi.org/10.3390/molecules200713384
26. Wang G, Zhu G, 2016. Molecular docking for drug discovery and development: a widely used approach but far from perfect. Future Medicinal Chemistry, 8(14): 1707-1710. https://doi.org/10.4155/fmc-2016-0143
27. Baranowska J, Kiss A, Szeleszczuk Ł, 2026. Molecular docking of natural compounds as DPP-4 inhibitors in type 2 diabetes: A comprehensive review. Pharmaceutics, 18(6): 741. https://doi.org/10.3390/pharmaceutics18060741
28. Hori H, Takayanagi T, Kamada Y, Shimoyoshi S, Ono Y, Kitagawa Y, Shibata H, Nagao M, Fujii W, Sakakibara Y, 2011. Genotoxicity evaluation of sesamin and episesamin. Mutation Research/Genetic Toxicology and Environmental Mutagenesis, 719(1-2): 21-28. https://doi.org/10.1016/j.mrgentox.2010.10.001
29. Medola JF, Cintra VP, Silva EPE, Royo VA, Silva R, Saraiva J, Albuquerque S, Bastos JK, Tavares DC, 2007. (-)-Hinokinin causes antigenotoxicity but not genotoxicity in peripheral blood of Wistar rats. Food and Chemical Toxicology, 45(4): 638-642. https://doi.org/10.1016/j.fct.2006.10.012
30. Hossain A, Rahman ME, Faruqe MO, Saif A, Suhi S, Zaman R, Hirad AH, Matin MN, Rabbee MF, Baek KH, 2024. Characterization of plant-derived natural inhibitors of dipeptidyl peptidase-4 as potential antidiabetic agents: A computational study.

Pharmaceutics, 16(4): 483. https://doi.org/10.3390/pharmaceutics16040483

31. Sajal H, Patil SM, Raj R, Shbeer AM, Ageel M, Ramu R, 2022. Computer-aided screening of phytoconstituents from Ocimum tenuiflorum against diabetes mellitus targeting DPP4 inhibition: A combination of molecular docking, molecular dynamics, and pharmacokinetics approaches. Molecules, 27(16): 5133. https://doi.org/10.3390/molecules27165133
32. Afolabi OB, Olasehinde OR, Olanipon DG, Mabayoje SO, Familua OM, Jaiyesimi KF, Agboola EK, Idowu TO, Obafemi OT, Olaoye OA, Oloyede OI, 2023. Antioxidant evaluation and computational prediction of prospective drug-like compounds from polyphenolic-rich extract of Hibiscus cannabinus L. seed as antidiabetic and neuroprotective targets: assessment through in vitro and in silico studies. BMC Complementary Medicine and Therapies, 23(1): 203. https://doi.org/10.1186/s12906-023-04023-7
33. Campbell SE, Stone WL, Whaley SG, Qui M, Krishnan K, 2003. Gamma tocopherol upregulates peroxisome proliferator activated receptor (PPAR) gamma expression in SW 480 human colon cancer cell lines. BMC Cancer, 3: 25. https://doi.org/10.1186/1471-2407-3-25
34. Sulaimon LA, Anise EO, Obuotor EM, Samuel TA, Moshood AI, Olajide M, Fatoke T, 2020. In vitro antidiabetic potentials, antioxidant activities and phytochemical profile of African black pepper (Piper guineense). Clinical Phytoscience, 6: 90. https://doi.org/10.1186/s40816-020-00236-2